

## SNAREs Prefer Liquid-disordered over “Raft” (Liquid-ordered) Domains When Reconstituted into Giant Unilamellar Vesicles\*<sup>§</sup>

Received for publication, June 23, 2004  
Published, JBC Papers in Press, June 29, 2004, DOI 10.1074/jbc.M407020200

Kirsten Bacia<sup>‡</sup>, Christina G. Schuette<sup>§</sup>, Nicoletta Kahya<sup>‡</sup>, Reinhard Jahn<sup>§</sup>, and Petra Schwille<sup>‡¶</sup>

From the <sup>‡</sup>Dresden University of Technology, Institute of Biophysics, Tatzberg 47-51, 01307 Dresden, Germany and <sup>§</sup>Department of Neurobiology, Max Planck Institute for Biophysical Chemistry, Am Fassberg 11, 37077 Goettingen, Germany

**Membrane domains (“rafts”) have received great attention as potential platforms for proteins in signaling and trafficking. Because rafts are believed to form by cooperative lipid interactions but are not directly accessible *in vivo*, artificial phase-separating lipid bilayers are useful model systems. Giant unilamellar vesicles (GUVs) offer large free-standing bilayers, but suitable methods for incorporating proteins are still scarce. Here we report the reconstitution of two water-insoluble SNARE proteins into GUVs without fusogenic additives. Following reconstitution, protein functionality was assayed by confocal imaging and fluorescence auto- and cross-correlation spectroscopy. Incorporation into GUVs containing phase-separating lipids revealed that, in the absence of other cellular factors, both proteins exhibit an intrinsic preference for the liquid-disordered phase. Although the picture from detergent resistance assays on whole cells is ambiguous, reconstitutions of components of the exocytic machinery into GUVs by this new approach should yield insight into the dynamics of protein complex associations with hypothesized liquid-ordered phase microdomains, the correspondence between detergent-resistant membranes and liquid-ordered phase, and the mechanism of SNARE-mediated membrane fusion.**

In 1988, Simons and van Meer (1) proposed a link between protein and lipid sorting in intracellular trafficking. They hypothesized that proteins destined for the apical membrane associate with glycosphingolipid-rich microdomains (termed “rafts”) in the trans-Golgi membrane held together by hydrogen bonding among the head groups. Microdomain formation is believed to be associated with a resistance against mild detergents (usually Triton X-100), providing a convenient read-out for whether a protein is in rafts. In polarized cells, rafts are sorted at the trans-Golgi-network into separate transport vesicles destined for the apical membrane, which explains the distinct protein and lipid compositions of apical and basolateral membranes. Examining Triton X-100 solubility of a glycosylphosphatidylinositol protein during transport from the endoplasmic reticulum to the plasma membrane, Brown and Rose (2) observed co-sorting of glycosphingolipids with apical but not basolateral proteins (2). Subsequently, liposomes were found to be insoluble in Triton X-100 if they contained lipids forming a

liquid-ordered ( $l_o$ )<sup>1</sup> phase, *i.e.* cholesterol in combination with sphingomyelin and saturated (3) phosphatidylcholine. These observations led to a view emphasizing cholesterol and ordered chain packing as the forces that hold the rafts together (4–6). Therefore, susceptibility to cholesterol depletion was introduced as an additional experimental tool to determine raft association.

Despite routine use of the Triton X-100 solubility assay, doubts persist as to whether detergent-resistant membranes (DRMs) correspond to  $l_o$  domains in intact membranes (7). Detergent application alters phase behavior (8), and DRM composition depends on the detergent used (9). Electron microscopy of isolated DRMs shows structures with a diameter of 0.1–1  $\mu\text{m}$  (2), which is larger than the estimated raft size in intact membranes (10), suggesting detergent-induced artifacts. Furthermore, cholesterol-dependent microdomains appear to be more heterogeneous than originally envisioned. For example, the apically sorted microvilli-localized protein, prominin, does not associate with classical DRMs prepared with Triton X-100 but associates with DRMs prepared with Lubrol and does so in a cholesterol-dependent manner (11). It is unclear how these microdomains relate to  $l_o$  and liquid-disordered ( $l_d$ ) phases, *i.e.* whether cholesterol-dependent clustering automatically implies an  $l_o$  phase.

Recently, evidence has been provided that SNARE proteins enrich in cholesterol-dependent microdomains in the plasma membrane (12, 13). SNARE proteins are vital components of intracellular fusion processes within the secretory pathway of eukaryotic cells. Their role as minimum machinery for membrane fusion was established by protein reconstitution into artificial liposomes, which were observed to undergo spontaneous fusion (14). The best studied are the SNAREs syntaxin 1, synaptobrevin 2, and SNAP-25 that are required for exocytosis of synaptic vesicles in neurons. The single-span transmembrane proteins, syntaxin 1 and synaptobrevin 2 (also referred to as VAMP2), are located on the plasma membrane and on the membrane of synaptic vesicles, respectively. The third partner, SNAP-25, is anchored to the plasma membrane by palmitoyl residues. SNAREs are characterized by a homologous stretch of 60–70 amino acids arranged in heptad repeats, which is referred to as the SNARE motif and is usually located directly adjacent to the membrane anchor domain. During membrane fusion, the SNARE motifs spontaneously assemble into a tight  $\alpha$ -helical bundle. According to the current view, the assembly of the SNARE motifs pulls the membranes closely together and initiates bilayer fusion (15–17).

\* The costs of publication of this article were defrayed in part by the payment of page charges. This article must therefore be hereby marked “advertisement” in accordance with 18 U.S.C. Section 1734 solely to indicate this fact.

<sup>§</sup> The on-line version of this article (available at <http://www.jbc.org>) contains Figs. S1–S4.

<sup>¶</sup> To whom correspondence should be addressed. Tel.: 49-351-463-40-328; Fax: 49-351-463-40-342; E-mail: [pschwil@gwdg.de](mailto:pschwil@gwdg.de).

<sup>1</sup> The abbreviations used are:  $l_o$ , liquid-ordered;  $l_d$ , liquid-disordered; FCS, fluorescence correlation spectroscopy; GUV, giant unilamellar vesicle; SUV, small unilamellar vesicle; DRM, detergent-resistant membrane; Syx, syntaxin; Syb, synaptobrevin; SNARE, soluble *N*-ethylmaleimide-sensitive factor attachment protein receptor; SNAP, soluble *N*-ethylmaleimide-sensitive factor attachment protein.

In the plasma membrane, syntaxin 1 forms microscopically visible clusters whose integrity is dependent on cholesterol (12, 18). Furthermore, syntaxin 1 can be cross-linked to a photoreactive cholesterol derivative, suggesting the association with cholesterol-dependent microdomains. Cholesterol removal profoundly inhibits exocytosis, suggesting that clustering is essential for SNARE function (12, 18). However, the syntaxin clusters do not co-localize with typical raft markers like glycosylphosphatidylinositol-linked proteins and syntaxin does not co-fractionate with DRMs (for review see Ref. 12 but also see Refs. 13 and 19 for an opposing view). The factors contributing to lateral membrane heterogeneities *in vivo* thus appear to be complex and experimentally difficult to characterize. In this light, we decided to single out the lipid phase aspect of rafts and determine the intrinsic protein affinity for the liquid-disordered or liquid-ordered phase in an artificial system. We have used GUV model membranes to investigate whether SNAREs partition into the  $l_o$  phase under the conditions of controlled composition and in the absence of detergent. Syntaxin and synaptobrevin were reconstituted into the “canonical raft mixture” of 1:1:1 C18-sphingomyelin, cholesterol, and dioleoyl-phosphatidylcholine (20, 21). A comparison with a classical  $l_o$  phase marker, GM1-bound cholera toxin, allowed the clear assignment to the  $l_d$  phase for both syntaxin 1A and synaptobrevin 2.

#### EXPERIMENTAL PROCEDURES

**Preparation of Recombinant SNARE Proteins**—Recombinant proteins were expressed and purified as previously described. Syntaxin 1A was expressed as a construct lacking the regulatory H<sub>abc</sub> domain and including a C-terminal cysteine for labeling (Syx H3, amino acids 183–289C (22)). Synaptobrevin 2 was expressed with an additional C-terminal cysteine (amino acids 1–117C (22)). Soluble synaptobrevin stands for the fragment of synaptobrevin 2 lacking the transmembrane domain and having a cysteine mutation (amino acids 1–96, 28C (23)). Soluble syntaxin describes the SNARE motif of syntaxin 1A (amino acids 180–262), carrying a cysteine mutation at position 252 (23).

Proteins were singly labeled at the indicated Cys residue with Alexa-488 maleimide (Molecular Probes) for transmembrane proteins or Cy5 maleimide (Amersham Biosciences) for soluble fragments (24). Additional cysteines were mutated to serine or were not accessible (cysteines in the transmembrane region (22)). In SNAP-25A, all of the cysteines were replaced by serines as described previously (25). It was not labeled.

**Reconstitution of SNARE Proteins into Small Liposomes**—Lipids obtained from Avanti Polar Lipids (GM1 from Calbiochem) were mixed in chloroform:methanol (2:1). Lipid mixture I consisted of brain phosphatidylcholine, brain phosphatidylethanolamine, brain phosphatidylserine, bovine liver phosphatidylinositol, and cholesterol at a molar ratio of 5:2:1:1:1. Lipid mixture II (domain-exhibiting membranes) contained dioleoyl-phosphatidylcholine, C18-sphingomyelin, cholesterol at a ratio of 1:1:1 and 0.1% ganglioside GM1. Lipids were dried and resuspended at a detergent to lipid ratio of 8:1 (mixture I) or 17:1 (mixture II) in buffer HB100 (20 mM Hepes/KOH, pH 7.4, 100 mM KCl, 1 mM dithiothreitol) containing 10% sodium cholate (Sigma). For lipid mixture II, heating in a waterbath was required until the mixture ceased to be turbid. Labeled SNARE proteins in HB100 containing 1.5% cholate were added to the detergent/lipid micelles to a final protein:lipid ratio of 1:300 or 1:60 (1.5  $\mu$ mol of total lipid). Proteoliposomes were formed by detergent removal on a Sephadex G-50 S column (volume ratio sample: column  $\leq$ 1:30), divided into five aliquots, snap-frozen in liquid nitrogen, and stored at  $-80^\circ\text{C}$ . Their diameter was  $\sim$ 25–35 nm (22). Using the same protocol but omitting the proteins, the vesicles were made from DLPC plus 0.0075% fluorescent marker (diIC<sub>18</sub>, Molecular Probes).

**Production of GUVs from Small Proteoliposomes**—A (proteo-)liposome aliquot was thawed, diluted in reconstitution buffer, pelleted by ultracentrifugation (200,000  $\times$  g, 90 min,  $4^\circ\text{C}$ ), and resuspended in 10  $\mu$ l of HB100. This concentrated liposome suspension was deposited as little droplets on an electrically conductive but optically transparent ITO coverslip (indium-tin-oxide-coated coverslip custom-made by GeSIM) to be used for GUV formation by electroswellling (26, 27). Residual water was evaporated in a vacuum at  $4^\circ\text{C}$  overnight. The ITO coverslip with the proteolipidic layer was assembled together with a second ITO coverslip into a flow-chamber of homemade design (based on Warner Instrument

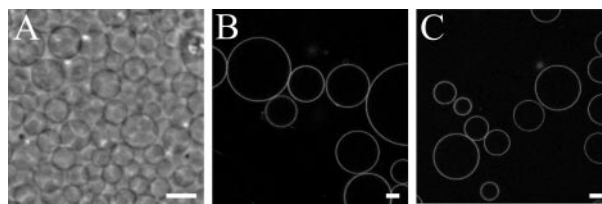


**FIG. 1. Imaging of SNARE-containing GUVs prepared from preformed SUVs.** GUVs containing fluorescently labeled synaptobrevin (A and B) and syntaxin (C) were visualized by phase-contrast (A) and confocal microscopy (B and C). The lipid composition consists of natural lipids (mixture I, see “Experimental Procedures”), which the scale bars define as 10  $\mu\text{m}$ . There is a high yield of spherical unilamellar GUVs, and protein incorporation is practically homogeneous.

Model RC 21), the chamber was filled with a 300 mM of sucrose solution, and a 1.2-V 10-Hz alternating electric field was applied to this capacitor-like configuration for 1–3 h. For lipid mixture II, GUVs were produced above the phase transition temperature (heating block or oven at  $\geq 65^\circ\text{C}$ ). GUVs were then allowed to cool down to room temperature, and the chamber was flushed with iso-osmolar phosphate-buffered saline buffer (Invitrogen). Soluble SNARE proteins were injected in phosphate-buffered saline at up to 16  $\mu\text{M}$  (SNAP-25), 1.6  $\mu\text{M}$  (Syx-Cy5), or 0.6  $\mu\text{M}$  (Syb-Cy5). For counterstaining, cholera toxin B subunit (Calbiochem) was labeled with monoreactive Cy5 NHS-ester (Amersham Biosciences) by standard methods and added to the chamber at 5  $\mu\text{g/ml}$  (cholera toxin B subunit-Cy5) in phosphate-buffered saline.

**Microscopy and Fluorescence Correlation Spectroscopy**—Microscopy and fluorescence correlation spectroscopy (FCS) were performed on a commercial ConfoCor 2 combination system (Carl Zeiss) (28). In confocal fluorescence imaging, spectral cross-talk was checked by performing separate scans with only single-laser excitations. FCS of diIC<sub>18</sub> used the configuration as described by Kahya *et al.* (27). Auto- and cross-correlation measurements (29) of Alexa-488 and Cy5-labeled proteins used essentially the configuration described by Bacia *et al.* (30). Calibration of the detection volumes yielded  $\omega_o = 0.17 \pm 0.01 \mu\text{m}$  for 543 nm and  $\omega_o = 0.15 \pm 0.01 \mu\text{m}$  for a 488-nm excitation. Laser powers were  $\leq$ 13 (488 nm) and 2 microwatts (543 nm). For these intensities and mobilities, photobleaching did not artifactually reduce diffusion times. Correlation curves  $G(\tau)$  were fitted appropriately by the FCS model equation for two-dimensional free Brownian diffusion (28) shown in Equation 1,

$$G(\tau) = \frac{1}{N_{\text{eff}}} \cdot \frac{1 - F + F \exp(-\tau/\tau_{\text{trip}})}{1 - F} \cdot \frac{1}{(1 + \tau/\tau_{\text{diff}})} + c \quad (\text{Eq. 1})$$

where  $N_{\text{eff}}$  denotes the number of fluorescent molecules in the detection volume, the second factor represents (triplet) blinking seen in the auto-correlation curves ( $F$ , triplet fraction;  $\tau_{\text{trip}}$ , triplet time), the third factor represents the diffusion term, and  $c$  is a constant accounting for slow fluctuations. The diffusion time ( $\tau_{\text{diff}}$ ) is related to the diffusion coefficient  $D$  by  $D = \omega_o^2/4\tau_{\text{diff}}$  where  $\omega_o$  is the  $1/e^2$  lateral radius of the detection volume. The means  $\pm$  S.D. of  $\tau_{\text{diff}}$  were calculated from measurements on multiple GUVs. Errors may also be estimated from visual inspection of the single measurements displayed in Supplemental Fig. S4.

#### RESULTS

**Production of SNARE-containing GUVs**—Normally, GUVs are prepared from a lipid solution in organic solvent that is thoroughly dried on an electrode. In search for a procedure that avoids exposure of the proteins to denaturing organic solvents, we found that vacuum drying of a concentrated, aqueous liposome suspension at  $4^\circ\text{C}$  on ITO-coated coverslips yields a lipid film that allows GUV formation by electroswellling. To examine whether there are any differences between GUVs prepared by both methods, we measured the lateral diffusion of the lipid analogue diIC<sub>18</sub> by FCS. No differences were detected (Supplemental Fig. S1). The liposome-based method was then applied to produce GUVs from small proteoliposomes prepared by detergent removal (Fig. 1A).

To test for protein aggregation, we visualized the reconstituted proteins by confocal microscopy and measured their mobilities by FCS. Fluorescence from the Alexa-488 labeled pro-

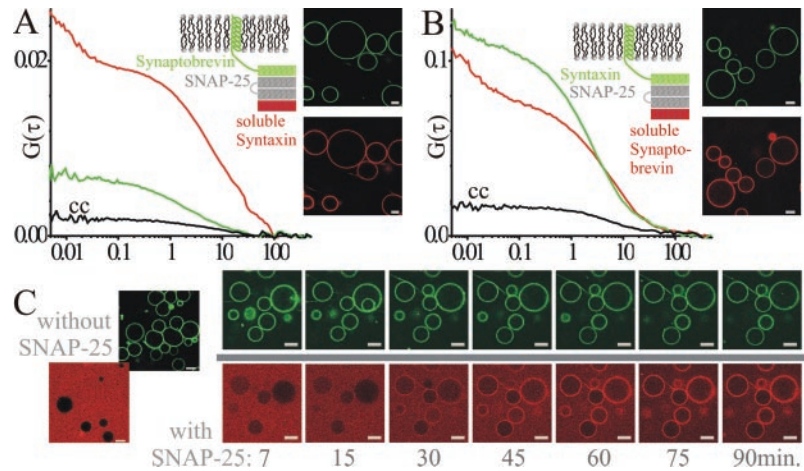


**FIG. 2. Specific binding of soluble SNARE motifs to proteins reconstituted in GUVs.** *A*, soluble syntaxin (labeled in red with Cy5) and soluble-unlabeled SNAP-25 were added to GUVs of lipid mixture I containing Alexa-488-labeled synaptobrevin (green). Co-localized red and green fluorescence at the membrane suggests binding. The positive cross-correlation amplitude (black curve) arises from concomitant diffusion of red, soluble, and green membrane-anchored protein. Laser intensities and particle ratios were optimized for low cross-talk. Cross-talk was quantified to contribute 4% to the cross-correlation amplitude (data not shown). Scale bars = 10  $\mu\text{m}$ . *B*, analogous experiment with incorporated syntaxin-Alexa-488 and soluble synaptobrevin-Cy5. Again, fluorescence is co-localized at the membrane and positive fluorescence cross-correlation shows specific binding. Cross-talk contributes 11% to the cross-correlation amplitude. *C*, binding of soluble syntaxin to synaptobrevin requires SNAP-25. *Left*, at 90 min after the addition of soluble syntaxin-Cy5, only fluorescence from unbound protein, but no membrane-localized red fluorescence, is observed. *Right*, in a time series after injection of unlabeled SNAP-25, membrane-localized red fluorescence starts to be visible because of the recruitment of labeled syntaxin. Syntaxin binding to synaptobrevin is known to require the presence of SNAP-25, thus confirming that binding is due to the formation of SNARE complexes on the membrane surface.

teins is confined to the membrane and is fairly uniform (Fig. 1, *B* and *C*). The proteo-GUV yield is high (Supplemental Fig. S3). FCS reveals complete diffusibility and indistinguishable diffusion coefficients for both single-span membrane proteins (synaptobrevin:  $D_{\text{Snb}} = (2.7 \pm 0.5) \times 10^{-8} \text{ cm}^2/\text{s}$ ; syntaxin:  $D_{\text{Snyx}} = (2.5 \pm 0.5) \times 10^{-8} \text{ cm}^2/\text{s}$ , Fig. 2 and Supplemental Fig. S4). A high mobility was also observed by fluorescence recovery after photobleaching (FRAP) (Supplemental Fig. S2). No singular large fluctuations are seen in the FCS count-rate traces, and correlation curves fit well to a two-dimensional, free Brownian diffusion model (data not shown, comparable with Fig. 3, *C* and *D*). Although these observations cannot rule out dimerization, for example (due to the weak dependence of the diffusion coefficient on the particle radius reflected in the Saffman-Delbruck equation (31)), they show that proteins become incorporated without any large-scale aggregation that would be expected if they were denatured during the reconstitution procedure.

To further test functional preservation, we assayed the binding of soluble SNARE motifs to the membrane-anchored proteins. Soluble red-labeled syntaxin and unlabeled SNAP-25 were added to GUVs containing green-labeled synaptobrevin. Analogously, soluble red-labeled synaptobrevin and SNAP-25 were added to green syntaxin-GUVs. In both experiments, co-localized fluorescence suggested binding (Fig. 2, *A* and *B*). Because at light optical image resolution unspecific binding to lipids cannot be excluded, specificity was investigated by dual-color cross-correlation spectroscopy. The positive cross-correlation amplitudes in Fig. 2, *A* and *B*, indicate specific co-diffusion of soluble and membrane-anchored SNARE proteins. Imaging alone can demonstrate specificity of binding here if the ternary nature of the complex is exploited (Fig. 2*C*). However, fluorescence cross-correlation is more versatile and can also assay specificity of binding in binary interactions.

**Reconstitution of SNARE Proteins into Phase-separating GUVs**—GUVs composed of dioleoyl-phosphatidylcholine:C18-sphingomyelin:cholesterol (1:1:1) are known to exhibit macroscopic phase separation (32). Domains can be visualized by marker enrichment. Fluorescent cholera toxin B subunit bound to the ganglioside GM1 (added at 0.1% to the lipid mixture) marks the  $l_o$  phase (21), whereas the lipid analogue diO (or the

structurally similar diI) become enriched in the  $l_d$  phase. Despite its enrichment in the  $l_d$  phase, FCS can assess diO mobility in both phases. diO diffusion is observed to be  $\sim 10$ -fold slower in the  $l_o$  compared with the  $l_d$  phase (Fig. 3, *E* and *F*). Thus, FCS offers a direct way of distinguishing lipid phases, which is independent of defining the  $l_o$  phase based on cholera toxin enrichment (27).

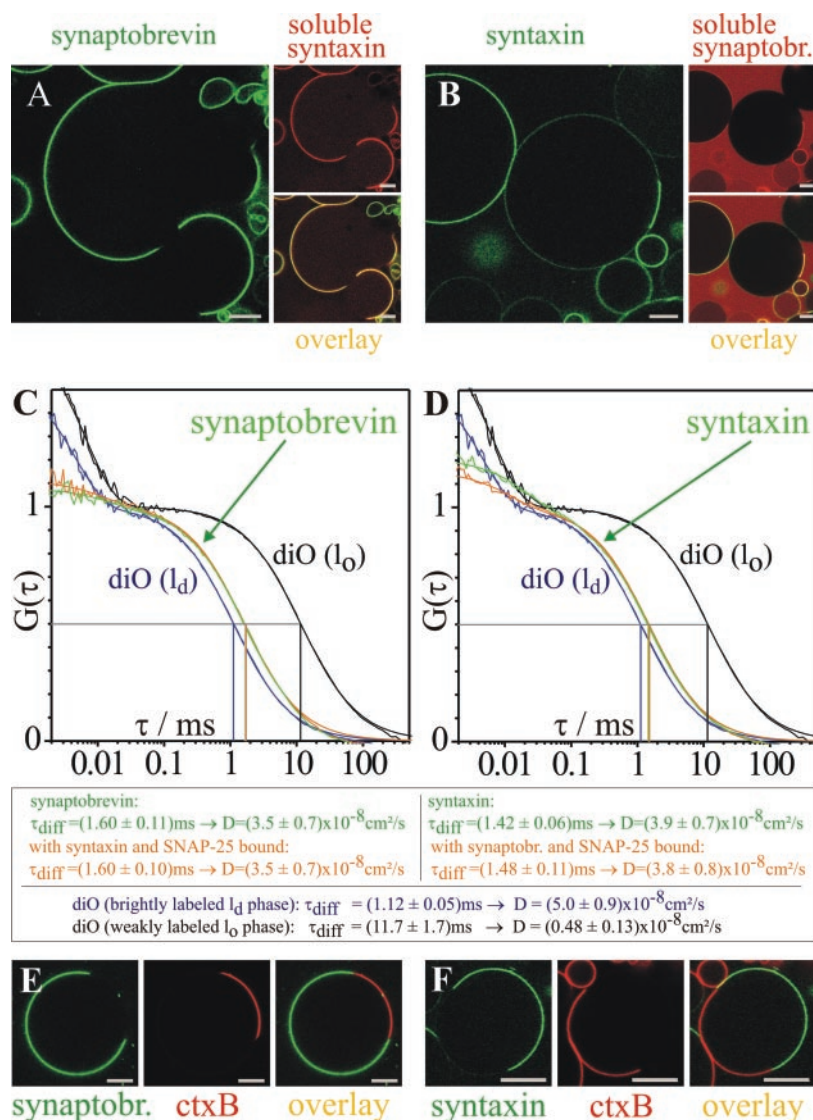
GUVs containing fluorescently labeled SNARE proteins were produced from liposomes of this lipid composition. Synaptobrevin and syntaxin display a clear preference for one phase, rendering only some regions of the GUV membranes as strongly labeled (Fig. 3, *A* and *B*, green channel). To identify the phases preferred by synaptobrevin and syntaxin, diffusional mobilities of both proteins in the strongly labeled phase were measured (Fig. 3, *C* and *D*, blue curves). They are identical within error and close to the diffusion of diO in the  $l_d$  phase (light gray curve). In contrast, diO diffusion in the  $l_o$  phase is  $\sim 7$ -fold slower (dark gray curve). Furthermore, cholera toxin B subunit (red), an established marker of rafts in cells and of  $l_o$  phase in model systems, exhibits a phase preference opposite to synaptobrevin (Fig. 3*E*) and syntaxin (Fig. 3*F*). We conclude that both synaptobrevin and syntaxin prefer the  $l_d$  phase. The binding of the soluble SNAREs does not significantly influence diffusion (orange curves in Fig. 3, *C* and *D*), suggesting that it does not alter phase behavior.

## DISCUSSION

We have used protein-containing GUVs prepared by a new mild method to determine the phase preference of unperturbed SNAREs in laterally segregating artificial membranes. Our data show that, in contrast to GM1-bound cholera toxin, both synaptobrevin 2 and syntaxin 1 partition in the  $l_d$  phase while being largely excluded from the  $l_o$  phase. We conclude that, although partitioning into  $l_o$  phase suffices to explain raft association of cholera toxin, cholesterol-dependent clustering of SNAREs *in vivo* is not explained by an intrinsic phase preference for the  $l_o$  phase. Furthermore, the proteins do not form large homo-oligomeric clusters as demonstrated by their diffusion coefficients, thus excluding homophilic interactions as an alternative explanation for SNARE clustering seen on a micro-

FIG. 3. **Syntaxin and synaptobrevin prefer the liquid-disordered phase.**

Scale bars = 10  $\mu\text{m}$ . The green channel images show synaptobrevin (A) and syntaxin (B) in GUVs produced from dioleoylphosphatidylcholine:C18-sphingomyelin:cholesterol (1:1:1) plus 0.1% GM1. Either protein shows a strong selective enrichment in one phase. Because part of the GUV preparation had to be carried out at elevated temperature, functional preservation of the proteins was evaluated again by the binding of the soluble SNARE counterparts (as in Fig. 2, A and B). Binding is specific, because fluorescence from the soluble SNAREs is only seen in membrane regions where incorporated SNAREs are enriched. C and D show normalized and averaged FCS curves (see Supplemental Fig. S4 for single experiment curves). Fitted and measured curves have the same colors. The diffusion of the incorporated SNAREs in their domains of enrichment is shown in green, and the diffusion of the lipid analogue diO in  $l_d$  and  $l_o$  phase is in blue and black, respectively. For both SNAREs, protein diffusion is only slightly slower (due to particle size) than diffusion of diO in the  $l_o$  phase. SNARE protein diffusion does not significantly change after the binding of soluble SNAREs (orange curves in C and E). Panels E and F show staining of synaptobrevin- and syntaxin-GUVs with Cy5-labeled cholera toxin B (ctxB) subunit, which is an  $l_o$  phase marker.



scopically visible scale in native membranes. The phase preferences of syntaxin and synaptobrevin (and even the definability of liquid-disordered and ordered phases) in a complex native biological membrane still remain an open question. However, the model system should allow the stepwise addition of biological complexity and an assessment of artificial perturbations. For instance, the effect of defined heterophilic protein interactions and detergent treatment on phase preference can be studied.

The fact that syntaxin is located mostly in the  $l_d$  domains agrees with a previous study in which syntaxin distribution was studied by atomic force microscopy in supported bilayers (33). In this preparation, syntaxin was not freely diffusible because it bound tightly to the mica support. This appears to be a general problem of supported membranes as reconstituted transmembrane proteins easily become immobilized or denatured by the solid support, limiting their usefulness for investigations requiring free diffusibility of proteins. Using a polymer cushion increases the distance to the support and avoids denaturation, but the polymer layer itself precludes free single-component Brownian diffusion of the protein (34).

Our data show that reconstitution of membrane proteins into GUVs with defined  $l_o$  state domains allows direct testing of the phase preference of a protein. However, the key problem is to integrate membrane proteins into GUVs while preserving their structural and functional integrity. Organic solvents generally

lead to protein denaturation (35), and the addition of the protein with detergent in the hydration step disrupts giant vesicle formation. Because membrane proteins can be readily reconstituted by detergent removal into SUVs, we sought to generate proteo-GUVs from a preparation of SUVs while avoiding protein denaturation. Our new procedure allows efficient formation of GUVs in good quality and with high protein concentration while preserving free single-component diffusion and functionality of the SNARE proteins. Although damage of sensitive proteins due to vacuum drying cannot be excluded, ongoing work indicates that a number of other membrane proteins can be functionally reconstituted as well.<sup>2</sup> Alternatively, proteo-GUVs can be generated by fusing protein-containing SUVs with preformed protein-free GUVs in aqueous media using a viral fusion peptide that is covalently linked to phospholipids in the proteoliposomes (36). Although this method is even milder than the one reported here, the presence of the fusion peptide makes such preparations unsuitable for functional studies of proteins involved in membrane fusion. Furthermore, it needs to be clarified whether the inclusion of the fusion peptide and a fusion-promoting cationic amphiphile affect the phase behavior of the system.

The use of advanced FCS on proteins reconstituted in GUVs

<sup>2</sup> N. Kahya and P. Schille, unpublished results.

opens up interesting avenues for further investigations. Cross-correlation spectroscopy has the advantage that it assesses diffusion (by auto-correlation) and binding (by cross-correlation) at the same time and for the same particles, thereby offering improved species discrimination compared with bulk experiments. GUVs are well suited to FCS and should also prove useful for related ultrasensitive optical techniques. We envision that conformational changes, oligomerization, and complex formation of membrane receptor proteins could be studied in GUVs using the latest FCS and FRET technologies. GUVs have recently become a popular tool for studying the phase behavior of lipid systems (27, 32, 37). The incorporation of proteins now adds a new dimension of complexity to these model membranes and may lead to new insights into membrane microorganization that are difficult to obtain through other approaches.

**Acknowledgments**—We thank members of the Schwille laboratory, in particular Dag Scherfeld and Inge Grueneberg, for their support of this work, the Carl Zeiss company for collaboration on FCS, and the Volkswagen Foundation for funding.

## REFERENCES

1. Simons, K., and van Meer, G. (1988) *Biochemistry* **27**, 6197–6202
2. Brown, D. A., and Rose, J. K. (1992) *Cell* **68**, 533–544
3. Schroeder, R., London, E., and Brown, D. (1994) *Proc. Natl. Acad. Sci. U. S. A.* **91**, 12130–12134
4. Simons, K., and Ikonen, E. (1997) *Nature* **387**, 569–572
5. Brown, D. A., and London, E. (1998) *J. Membr. Biol.* **164**, 103–114
6. Schroeder, R. J., Ahmed, S. N., Zhu, Y., London, E., and Brown, D. A. (1998) *J. Biol. Chem.* **273**, 1150–1157
7. Munro, S. (2003) *Cell* **115**, 377–388
8. Heerklotz, H. (2002) *Biophys. J.* **83**, 2693–2701
9. Schuck, S., Honsho, M., Ekroos, K., Shevchenko, A., and Simons, K. (2003) *Proc. Natl. Acad. Sci. U. S. A.* **100**, 5795–5800
10. Simons, K., and Toomre, D. (2000) *Nat. Rev. Mol. Cell. Biol.* **1**, 31–39
11. Roper, K., Corbeil, D., and Huttner, W. B. (2000) *Nat. Cell Biol.* **2**, 582–592
12. Lang, T., Bruns, D., Wenzel, D., Riedel, D., Holroyd, P., Thiele, C., and Jahn, R. (2001) *EMBO J.* **20**, 2202–2213
13. Chamberlain, L. H., Burgoyne, R. D., and Gould, G. W. (2001) *Proc. Natl. Acad. Sci. U. S. A.* **98**, 5619–5624
14. Weber, T., Zemelman, B. V., McNew, J. A., Westermann, B., Gmachl, M., Parlati, F., Sollner, T. H., and Rothman, J. E. (1998) *Cell* **92**, 759–772
15. Chen, Y. A., and Scheller, R. H. (2001) *Nat. Rev. Mol. Cell. Biol.* **2**, 98–106
16. Jahn, R., Lang, T., and Sudhof, T. C. (2003) *Cell* **112**, 519–533
17. Rizo, J., and Sudhof, T. C. (2002) *Nat. Rev. Neurosci.* **3**, 641–653
18. Ohara-Imaizumi, M., Nishiwaki, C., Kikuta, T., Kumakura, K., Nakamichi, Y., and Nagamatsu, S. (2004) *J. Biol. Chem.* **279**, 8403–8408
19. Xia, F., Gao, X., Kwan, E., Lam, P. P., Chan, L., Sy, K., Sheu, L., Wheeler, M. B., Gaisano, H. Y., and Tsushima, R. G. (2004) *J. Biol. Chem.* **279**, 24685–24691
20. Samsonov, A. V., Mihalyov, I., and Cohen, F. S. (2001) *Biophys. J.* **81**, 1486–1500
21. Dietrich, C., Volovyk, Z. N., Levi, M., Thompson, N. L., and Jacobson, K. (2001) *Proc. Natl. Acad. Sci. U. S. A.* **98**, 10642–10647
22. Schuette, C. G., Hatsuzawa, K., Margittai, M., Stein, A., Riedel, D., Kuster, P., Konig, M., Seidel, C., and Jahn, R. (2004) *Proc. Natl. Acad. Sci. U. S. A.* **101**, 2858–2863
23. Margittai, M., Fasshauer, D., Pabst, S., Jahn, R., and Langen, R. (2001) *J. Biol. Chem.* **276**, 13169–13177
24. Pabst, S., Margittai, M., Vainius, D., Langen, R., Jahn, R., and Fasshauer, D. (2002) *J. Biol. Chem.* **277**, 7838–7848
25. Fasshauer, D., Eliason, W. K., Brunger, A. T., and Jahn, R. (1998) *Biochemistry* **37**, 10354–10362
26. Angelova, M. I., and Dimitrov, D. S. (1986) *Faraday Discuss. Chem. Soc.* **81**, 303–311
27. Kahya, N., Scherfeld, D., Bacia, K., Poolman, B., and Schwille, P. (2003) *J. Biol. Chem.* **278**, 28109–28115
28. Bacia, K., and Schwille, P. (2003) *Methods* **29**, 74–85
29. Schwille, P., Meyer-Almes, F. J., and Rigler, R. (1997) *Biophys. J.* **72**, 1878–1886
30. Bacia, K., Majoul, I. V., and Schwille, P. (2002) *Biophys. J.* **83**, 1184–1193
31. Saffman, P. G., and Delbruck, M. (1975) *Proc. Natl. Acad. Sci. U. S. A.* **72**, 3111–3113
32. Dietrich, C., Bagatolli, L. A., Volovyk, Z. N., Thompson, N. L., Levi, M., Jacobson, K., and Gratton, E. (2001) *Biophys. J.* **80**, 1417–1428
33. Saslowsky, D. E., Lawrence, J. C., Henderson, R. M., and Edwardson, J. M. (2003) *J. Membr. Biol.* **194**, 153–164
34. Wagner, M. L., and Tamm, L. K. (2000) *Biophys. J.* **79**, 1400–1414
35. Tanford, C. (1968) *Adv. Protein Chem.* **23**, 121–282
36. Kahya, N., Pecheur, E. I., de Boeij, W. P., Wiersma, D. A., and Hoekstra, D. (2001) *Biophys. J.* **81**, 1464–1474
37. Veatch, S. L., and Keller, S. L. (2002) *Phys. Rev. Lett.* **89**, 268101